JCTC Journal of Chemical Theory and Computation

Weakly Bonded Complexes of Aliphatic and Aromatic Carbon Compounds Described with Dispersion Corrected Density Functional Theory

Enrico Tapavicza, I-Chun Lin, O. Anatole von Lilienfeld,[‡] Ivano Tavernelli, Maurício D. Coutinho-Neto,[§] and Ursula Rothlisberger*

Laboratoire de Chimie et Biochimie Computationelle, Ecole Polytechnique Fédérale de Lausanne (EPFL), 1015 Lausanne, Switzerland

Received March 1, 2007

Abstract: Interaction energies and structural properties of van der Waals complexes of aliphatic hydrocarbons molecules and crystals of aromatic hydrocarbon compounds are studied using density functional theory augmented with dispersion corrected atom centered potentials (DCACPs). We compare the performance of two sets of DCACPs, (a) DCACP-MP2, a correction for carbon only, generated using MP2 reference data and a penalty functional that includes only equilibrium properties and (b) DCACP-CCSD(T), a set that has been calibrated against CCSD(T) reference data using a more elaborate penalty functional that explicitly takes into account some long-range properties and uses DCACP corrections for hydrogen and carbon atoms. The agreement between our results and high level ab initio or experimental data illustrates the transferability of the DCACP scheme for the gas and condensed phase as well as for different hybridization states of carbon. The typical error of binding energies for gas-phase dimers amounts to 0.3 kcal/mol. This work demonstrates that only one DCACP per element is sufficient to correct for weak interactions in a large variety of systems, irrespective of the hybridization state.

1. Introduction

London dispersion forces are fundamental for the proper description of chemical and biological systems such as molecular liquids and crystals, proteins, and nucleic acids. Since these forces are purely due to electron correlation effects, they are difficult and computationally expensive to capture using conventional quantum chemical approaches. Kohn−Sham density functional theory (DFT)[1,2] is a very popular first principles electronic structure method due to its relatively high accuracy and low computational cost. DFT is in principle exact and should correctly describe the London dispersion forces if the true exchange-correlation (xc) functional were known. However, most of the conventional local approximations to xc-functionals are unable to describe dispersion reliably.[3−6] To account for these forces in DFT, several remedies have been proposed and implemented, for example, prepartitioning of the electron density,[7] solving the adiabatic connection formula for the long-range part of the interaction energy,[8] using symmetry adapted perturbation theory,[9,10] developing more sophisticated approximations to the xc-potential,[11,12] or adding an explicit dispersion term with a C_6 coefficient determined either empirically[5,13,14] or generated by the instantaneous dipole moment of the exchange hole.[15−17]

Recently, dispersion corrected atom centered potentials (DCACPs) have been introduced to account for London dispersion forces within self-consistent DFT calculations and have been shown to perform remarkably well for several cases.[18−21] Here, we systematically probe the transferability of DCACPs to various hybridization states other than the one used in the calibration and test their performance for

* Corresponding author e-mail: ursula.roethlisberger@epfl.ch, http://lcbcpc21.epfl.ch.

‡ Current address: Department of Chemistry, New York University, New York, NY 10003.

§ Current address: Centro de Ciências Naturais e Humanas, Universidade Federal do ABC, Rua Santa Adélia, 166 Santo André, São Paulo, Brazil BR-09.210-170.

10.1021/ct700049s CCC: $37.00
Published on Web 08/08/2007

some solid-state systems. In addition we compare the performance of two generations of DCACPs, which differ in their reference method and in their calibration procedure. The study focuses on carbon which, in the case of biomolecular classical force fields, is the element that requires the largest number of different atom types, i.e., it requires very different Lennard-Jones coefficients for different hybridization states.[22] In stark contrast, in the DCACP approach only one carbon DCACP is employed for all hybridization states. The question we pose in this study is with which accuracy this large variety of systems can be described in spite of the limitation to a single effective potential. We study several weakly bonded complexes of carbon compounds using two sets of DCACPs previously calibrated against MP2 (DCACP-MP2[18]) and CCSD(T) (DCACP-CCSD(T)[23]) references, respectively. The performance of DCACPs for different hybridization states is investigated by studying a series of aliphatic hydrocarbon C_2H_n ($n = 2,4,6$) homo dimers as well as the methane−ethene hetero dimer in the gas phase. Moreover, we assess the transferability of DCACPs from the gas to the condensed phase for crystals of benzene and graphite. Our results suggest that DCACPs offer a cheap, pragmatic way to include the effect of London dispersion forces in DFT calculations that is strongly transferable, i.e., once calibrated, the same DCACP for each element can be employed in different hybridization states without additional tuning.

2. Computational Details

All DFT calculations were carried out with the plane wave code CPMD,[24,25] the xc-functional BLYP,[26,27] and pseudopotentials of Goedecker et al.[28] Two generations of DCACPs, DCACP-MP2[18] and DCACP-CCSD(T),[23] were employed in this study. These two sets differ in the following three respects: (a) the chosen reference during the calibration stage (MP2 for DCACP-MP2 and CCSD(T) for DCACP-CCSD(T)); (b) a 'united atom' approach for DCACP-MP2, i.e., only carbon atoms are corrected by a DCACP but not hydrogens, whereas DCACPs for both hydrogen and carbon have been used in DCACP-CCSD(T); and (c) for DCACP-MP2, the penalty functional included only the energy and forces at equilibrium distance,[18] whereas a new penalty functional was introduced to improve the description of the intermolecular midrange to long-range behavior in the calibration of the DCACP-CCSD(T) set.[29] The DCACPs were calibrated to correct the BLYP xc functional. Further details of the calibration of the two generations of DCACPs can be found in refs 18 and 29. For comparison purposes, standard BLYP calculations without dispersion correction were also carried out.

In order to calculate the interaction energy of the gas-phase dimers, the monomer geometry was first optimized using the pure BLYP functional. The BLYP optimized monomer geometries were then used to construct the dimers in all calculations. The dimer geometries of ethane, ethene, and ethyne shown in Figure 1 were placed in an isolated cell with dimensions $25 \times 10 \times 10$ Å^3. A plane wave cutoff of 100 Ry was applied. For the methane−ethene complex, a cell measuring $26 \times 13 \times 12$ Å ^{3} and a plane wave cutoff of 150 Ry was used. In all cases the intermolecular distance was varied along the *x*-axis. The orientation of the methane−ethene complex is indicated by the coordinate system in Figure 1. The interaction energies, defined as $E_{AB}^{int} = E_{AB}^{total} - E_A^{total} - E_B^{total}$, were calculated at various distances. In order to gauge the accuracy of the dispersion corrected DFT calculations, the corresponding MP2 and CCSD(T) calculations have been carried out using the ab initio program packages GAUSSIAN03[30] or MOLPRO.[31]

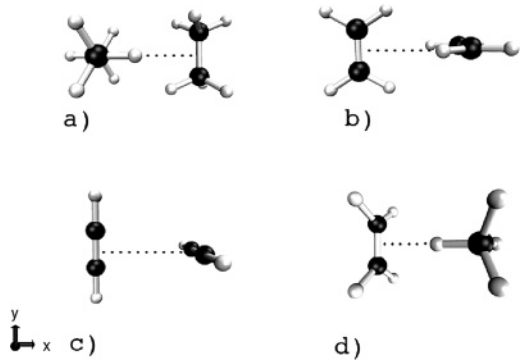

Figure 1. Geometries of the hydrocarbon dimers: (a) $(C_2H_6)_2$, (b) $(C_2H_4)_2$, (c) $(C_2H_2)_2$, and (d) $C_2H_4\cdots CH_4$. The intermolecular distance refers to the distance between the midpoints of the C−C bonds of the two molecules in the case of C_2H_n. In case of the $CH_4-C_2H_4$ complex, it is defined as the distance between the midpoint of the C−C bond in ethene and the hydrogen atom of methane pointing toward the ethene molecule.

The MP2 and CCSD(T) calculations were done at the same intermolecular distances with the monomers fixed at the BLYP optimized geometry. In both sets of calculations the aug-cc-pVTZ basis set and counterpoise corrections[32,33] were employed.

Calculations for the benzene crystal were based on the experimentally determined space group P_{bca}.[34,35] Total energy calculations were performed by isotropically varying the volume of a unit cell, whereas the internal coordinates of the four monomers were allowed to relax. The total energy of the monomer (E_{mono}^{total}) was calculated in an isolated cubic supercell with an edge of 12 Å. The cohesive energy of the benzene crystal was then calculated using $E^{cohesive} = [E_{cryst}^{total} - 4*E_{mono}^{total}]/4$. A plane wave cutoff of 200 Ry was enough to ensure converged results with respect to the number of plane waves caused by the variation of the unit cell volume.[36]

For the determination of the interlayer binding (IB) energy of graphite, a monomeric graphene sheet containing 32 carbon atoms was geometry optimized under two-dimensional periodic boundary conditions (PBC) along the graphene plane (*xy*). Thereafter, the total energy of 3 sheets (96 atoms) in ABA and ABC packing was calculated with various interlayer distances while keeping the internal geometry of the layers rigid. A cell with dimensions $9.84 \times 8.52 \times 24.0$ Å^3 (two-dimensional PBC along *x* and *y*) and a plane wave cutoff of 100 Ry were used. The IB energy per atom was calculated as E_{IB} (ABC)/atom $= [E_{total}$ (ABC) $- 3*E_{total}$ (A)]/64, where atoms in the first and third layer were counted as 'half' to allow for direct comparison to the corresponding result for the crystal.

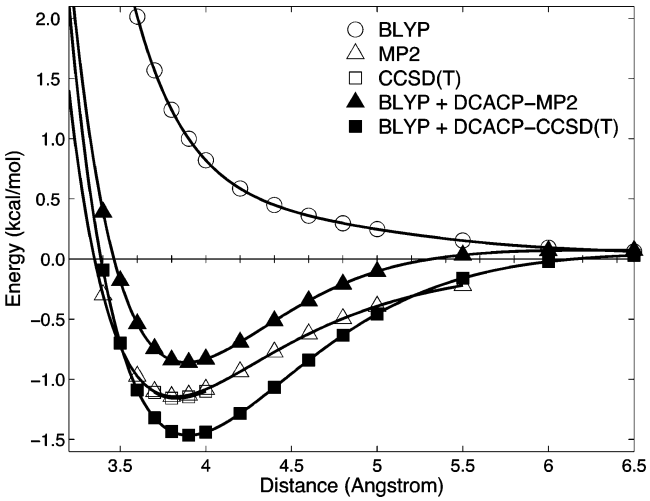

Figure 2. Interaction energy [kcal/mol] of the ethane dimer as a function of the intermolecular distance [Å]. For the definition of the intermolecular distance see the caption of Figure 1.

Table 1. Summary of the Calculations for the Gas-Phase Dimers[a]

	DCACP-MP2		MP2		Δ	
	E^{int}	r_{eq}	E^{int}	r_{eq}	E^{int}	r_{eq}
$(C_2H_6)_2$	−0.859	3.88	−1.145	3.82	0.286	0.06
$(C_2H_4)_2$	−1.287	3.79	−1.476	3.72	0.189	0.07
$(C_2H_2)_2$	−0.523	3.83	−0.295	3.98	−0.228	−0.15
$C_2H_4\cdots CH_4$	−0.385	3.08	−0.520	3.12	0.135	−0.04
MD					0.096	−0.02
MAD					0.209	0.08
	DCACP-CCSD(T)		CCSD(T)		Δ	
	E^{int}	r_{eq}	E^{int}	r_{eq}	E^{int}	r_{eq}
$(C_2H_6)_2$	−1.464	3.90	−1.158	3.83	−0.306	0.07
$(C_2H_4)_2$	−1.301	3.94	−1.390	3.75	0.089	0.19
$(C_2H_2)_2$	−0.135	4.15	−0.154	4.17	0.019	−0.02
$C_2H_4\cdots CH_4$	−0.547	3.09	−0.50[b]	3.12[b]	−0.047	−0.02
MD					0.061	0.06
MAD					0.115	0.08

[a] Equilibrium distances (r_{eq} [Å]) and binding energies at equilibrium distance (E^{int} [kcal/mol]) are shown together with the deviations (Δ) from the reference of the corresponding level of theory. The definitions of the labels 'MD' and 'MAD' are given in the text. [b] Values are taken from ref 38.

3. Results

The resulting potential energy curves of the DFT calculations for the hydrocarbon dimers are shown in Figures 2−5. The reference values of the equilibrium distances of the reference methods are also shown. As observed in refs 5 and 37, uncorrected BLYP results in a purely repulsive interaction energy for all vdW dimers studied and converges to zero in the dissociative limit (Figures 2−5). The equilibrium distances and binding energies for the dimers obtained with the two sets of DCACPs are summarized in Table 1. Mean deviations (MD), defined as $(1/N)(x^{DCACP} - x^{ref})$, and mean absolute deviations (MAD), defined as $(1/N)|x^{DCACP} - x^{ref}|$, for characteristic properties are also given. Here, N is the number of test systems, and x^{DCACP} and x^{ref} are the equilibrium distance or the binding energy at the equilibrium distance of the DCACP calculations and the reference calculations. Always the same level of theory which was used in the calibration for the DCACPs was chosen as reference. It should be mentioned that except for the ethyne dimer, MP2/aug-cc-pVTZ and CCSD(T)/aug-cc-pVTZ reference values differ by less than 0.1 kcal/mol for the binding energy at equilibrium distance and predict the same equilibrium distances within 0.05 Å (Table 1, Figures 2, 3, and 5).

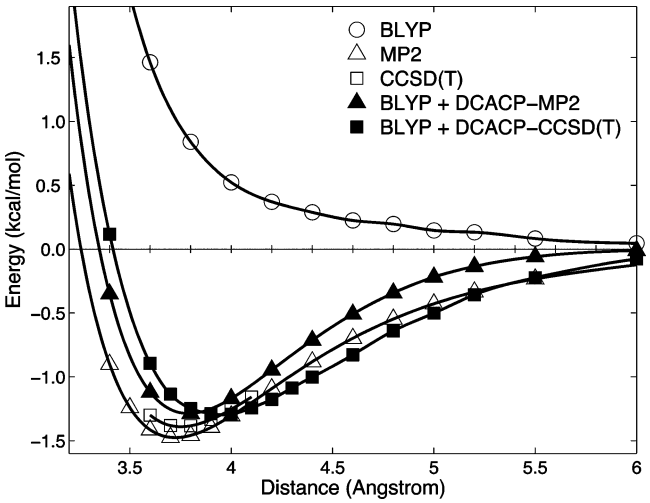

Figure 3. Interaction energy [kcal/mol] of the ethene dimer as a function of the intermolecular distance [Å]. For the definition of the intermolecular distance see the caption of Figure 1.

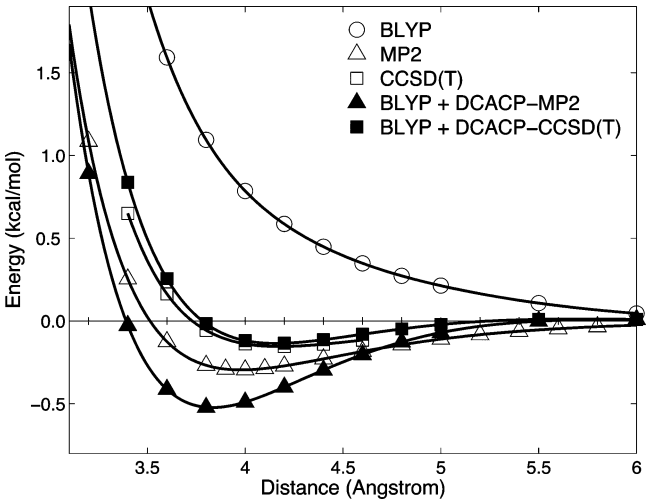

Figure 4. Interaction energy [kcal/mol] of the ethyne dimer as a function of the intermolecular distance [Å]. For the definition of the intermolecular distance see the caption of Figure 1.

The DCACP-MP2 corrected DFT calculations predict equilibrium distances within 0.08 Å of the corresponding MP2 calculations for all dimers except for $(C_2H_2)_2$ where a maximal deviation of 0.15 Å is found. However, ethyne dimer exhibits a very flat potential energy surface (PES) around the minimum (Figure 4), and the deviation of 0.15 Å corresponds to a maximal variation in the energy of only

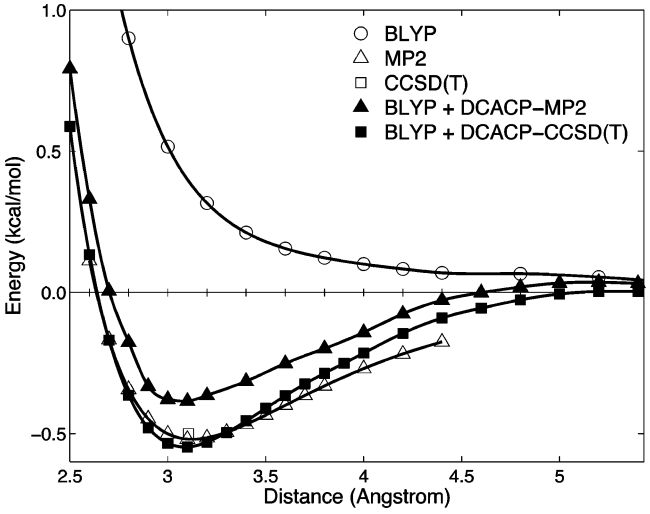

Figure 5. Interaction energy [kcal/mol] of the methane−ethene complex as a function of the intermolecular distance [Å]. The reference value was obtained with basis set extrapolated CCSD(T) calculations.[38] For the definition of the intermolecular distance see the caption of Figure 1.

0.05 kcal/mol, therefore, a higher tolerance in the prediction of the equilibrium distances is acceptable.

The DCACP-MP2 MAD for interaction energies amounts to 0.209 kcal/mol at the equilibrium distance, where the largest deviation of 0.286 kcal/mol is found in the case of $(C_2H_6)_2$.

Using the DCACP-CCSD(T) set, intermolecular equilibrium distances are predicted with similar accuracy with a MAD of 0.08 Å. The largest deviation of 0.19 Å is exhibited by the ethene dimer, which is larger than in the corresponding DCACP-MP2 result. The larger deviation in the prediction of the equilibrium distance in the case of ethene can be explained by the use of the second parameter in the penalty functional in the calibration of the DCACP-CCSD(T), which accounts for a better description of the slope of the PES around the minimum. The DCACP-MP2 predict the minimum distance of the ethene dimer with smaller deviation from the reference, but, compared to MP2, the resulting PES is too steep around the minimum and approaches the asymptotic limit too fast. In contrast the shape of DCACP-CCSD(T) PES is flatter, and the slope is similar to the CCSD(T) reference curve. The binding energy of the ethene dimer is very well reproduced with an error of only 0.089 kcal/mol.

In the case of the hetero dimer (methane−ethene) MP2 and CCSD(T) both predict similar interaction energies and equilibrium distances (Figure 5). Both DCACP sets reproduce very well the equilibrium distance (Table 1), but the interaction energy is more accurately predicted by the DCACP-CCSD(T). This is probably due to the use of an extra DCACP for hydrogen in the case of DCACP-CCSD(T), which is especially important for the case of the methane−ethene dimer, where a hydrogen of methane is pointing toward the ethylene molecule (Figure 1).

On average, the same accuracy is found between DCACP-MP2 and DCACP-CCSD(T) calculations with respect to the reference equilibrium distances which are predicted with an MAD of 0.08 Å, while the MAD of the DCACP-CCSD(T) interaction energies of 0.115 kcal/mol is slightly smaller than in the case of DCACP-MP2.

The better correlation between dispersion corrected DFT and the reference in the case of DCACP-CCSD(T) is presumably due to the separate calibration of hydrogen and carbon and the improved midrange and long-range behavior.[29] However, by construction in both cases, the DCACP interaction energies approach the dispersion uncorrected BLYP values because at large distances the effect of the DCACPs vanishes.[29] For the systems studied here, for distances typically larger than 5.5 Å the DCACPs correction approaches zero, and the corrected and uncorrected potentials converge to the same value. In general in all the discussed dimer interaction curves it can be seen that the DCACP-CCSD(T) PES approach the asymptotic limit (BLYP PES) more slowly than the first generation of DCACPs, which are based solely on a equilibrium penalty functional.

Comparing the deviations of the two DCACPs from the corresponding reference values for the four different dimers (Table 1), it can be seen that they differ in magnitude and that also the sign of the deviation can be different (e.g., Figure 2). For example, in case of the ethane dimer the reference values of MP2 and CCSD(T) are almost equal, but the DCACP-MP2 underestimates the binding energy while the DCACP-CCSD(T) overestimates it. This can be explained because of the different calibration procedures and because of the fact that in the case of DCACP-MP2 only the DCACP for carbon was used, while in DCACP-CCSD(T) simultaneous DCACPs for carbon and hydrogen atoms were included. The latter is especially important for cases in which the carbon−hydrogen ratio differs from the one of the calibration system. Therefore it cannot be expected that the deviation from the reference curve has the same sign and magnitude for the two generations of DCACPs.

To further probe the transferability of DCACPs to different hybridization states and to assess their long-range behavior, we also have studied the molecular crystal of benzene. With DCACP-MP2, a very shallow minimum (6.2 kcal/mol) is predicted at a ratio of 0.91 between the theoretical and the experimental density (ρ/ρ_{exp}) (Figure 6). Experimental cohesive energies for the benzene crystal range from values of 9.0−12.5 kcal/mol.[39−42] A better agreement with experimental results is obtained when DCACP-CCSD(T) are used. In this case the cohesive energy is evaluated as 12.1 kcal/mol, within the spread of experimental values. In addition, the predicted equilibrium density of the unit cell is at 0.95 times the experimental density, slightly closer to the experiment than the unit cell density predicted by DCACP-MP2. The underestimation of the binding energy of DCACP-MP2 compared to DCACP-CCSD(T) is probably due to its worse description in the midrange to long-range regime. In the case of DCACP-CCSD(T) where an additional term was introduced in the penalty functional, the description of this range is improved.[29]

Another test for the transferability to the solid state was carried out by investigating the relative stability of different graphite configurations. Graphite exists in a thermodynamic stable hexagonal (AB) and a metastable rhombohedral

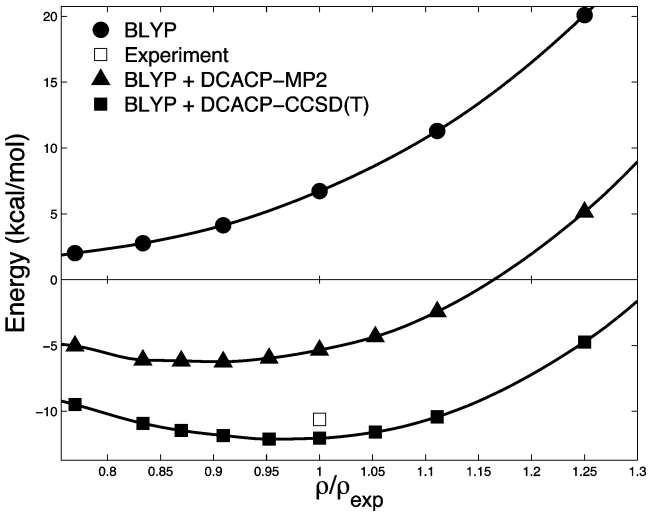

Figure 6. Cohesive binding energy of the benzene crystal [kcal/mol] as a function of the ratio between the calculated density ρ and the experimental density ρ_{exp}. The experimental value (10.6 kcal/mol) recommended for comparison in ref 42 is plotted for comparison.

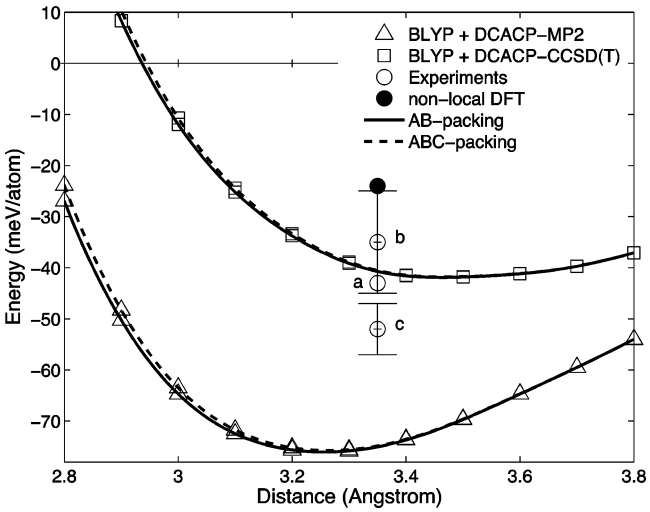

Figure 7. Interlayer binding energy [meV/atom] of three graphene sheets as a function of the interlayer distance [Å]. The experimental values (circle) of Girifalco et al. (a),[43] Benedict et al. (b),[44] and Zacharia et al. (c)[45] are plotted at the experimental interlayer distance of 3.35 Å according to ref 48. The experimental uncertainties, if available, are indicated by the error bars. A theoretical result from a recent nonlocal DFT calculation[49] is also shown as a filled circle.

configuration (ABC). In Figure 7, the IB energies for AB and ABC packing, obtained with the two sets of DCACPs, are shown. While both sets of DCACPs predict the ABC packing to be less favorable than the AB packing, consistent with the experimental observations, the difference in the IB energies between ABC and AB packing is at the limit of the numerical precision of this study. It is worth noting that the energy difference between the two configurations increases at short range and approaches zero in the dissociation limit.

Concerning absolute binding energies of hexagonal graphite, three different experimental IB energies exist in the literature for comparison: in the earliest publication, an IB energy of 43 meV/atom was measured.[43] More recent studies estimated IB energies to be 35 ± 10[44] and 52 ± 5[45] meV/atom. DCACP-MP2 corrected DFT predicts an IB energy of $\cong$76 meV/atom,[47] a clear overestimation with respect to all available experimental data, which is consistent with the fact that MP2 overestimates the binding of the benzene dimer.[46] DCACP-CCSD(T) predicts a binding energy of approximately 42 meV/atom agreeing within less than 10 meV/atom with all experimental values. However, the equilibrium interlayer distance of 3.30 Å predicted by the DCACP-MP2 calculations is slightly closer to the experimental value of 3.35 Å than the distance of 3.45 Å predicted by the DCACP-CCSD(T) calculations. As shown in Figure 7 DCACP-CCSD(T) predicts a flatter PES around the equilibrium distance.

4. Conclusion

Using dispersion corrected and uncorrected DFT, structures and interaction energies of dispersion dominated systems such as the dimers of ethane, ethene, ethyne, and the methane−ethene dimer were computed. For the hydrocarbon dimers, both DCACP-MP2 and DCACP-CCSD(T) predict the equilibrium intermolecular separations within a MAD of 0.08 Å to the corresponding reference values, and interaction energies of the dimers are predicted within a MAD of 0.209 and 0.115 kcal/mol, respectively. DCACPs exhibit good transferability with respect to all hybridization states (sp^3 to sp), where the typical maximum error for interaction energies and equilibrium distances amounts to 0.3 kcal/mol and 0.2 Å, respectively. For the gas-phase dimers, DCACP-CCSD(T) results correlate on average better with the corresponding post-Hartree−Fock results than the DCACP-MP2 set.

Furthermore, the transferability of DCACPs to the condensed phase has been investigated. Both sets of DCACPs drastically improve the description of crystals compared to the uncorrected BLYP results, which predict the crystals of benzene and graphite to be unstable.

For the benzene crystal, a qualitatively good description is obtained using the DCACP-MP2 set, and a highly accurate description is obtained with DCACP-CCSD(T). The latter predicts a cohesive energy which lies in the range of experimental values, and the density of the crystal is predicted within 5% of the experimental density.

Considering graphite, the DCACP-CCSD(T) IB energy is in very good agreement with the experiments, whereas DCACP-MP2 overestimates the IB energy. As in the case of benzene, the use of DCACPs generally leads to a drastic improvement of the calculated IB energies and geometries compared to conventional BLYP.

In summary, in the studied cases DCACPs lead to a clear improvement in the description of dispersion effects with respect to pure BLYP DFT and in most cases provide excellent results compared to high level ab initio data or experiments. A clear advantage of this method over empirical atom−atom corrections is its high transferabilty, i.e., a single DCACP per element is sufficient to account for weak interactions in various chemical environments.

The DCACP-CCSD(T) set, in general, leads to a better agreement with the corresponding reference data than DCACP-MP2, especially in the solid phase where long-range interactions are of high importance. The better performance of the DCACP-CCSD(T) can be attributed to an improved calibration procedure for a better description of the mid- to long-range interactions and to a separate calibration of hydrogen and carbon atoms. In addition, CCSD(T) is of higher accuracy than MP2. We therefore suggest the use of DCACP-CCSD(T) in DFT applications where dispersion forces are of importance.

Acknowledgment. The authors acknowledge discussions with Michele Parrinello and Ari P. Seitsonen. This work was supported by the Swiss National Science Foundation (Grant No. 200020-108063/1) and BIOMACH, Priority 3 (NMP-2002-3.4.1.1-3: Contract No. 505487-1).

Supporting Information Available: Geometries and parameters of the DCACP-CCSD(T). This material is available free of charge via the Internet at http://pubs.acs.org.

References

(1) Hohenberg, P.; Kohn, W. *Phys. Rev.* **1964**, *136*, B864.

(2) Kohn, W.; Sham, L. J. *Phys. Rev.* **1965**, *140*, A1133.

(3) Kristyán, S.; Pulay, P. *Chem. Phys. Lett.* **1994**, *229*, 175.

(4) Pérez-Jordá, J. M.; Becke, A. D. *Chem. Phys. Lett.* **1995**, *233*, 134.

(5) Meijer, E. J.; Sprik, M. *J. Chem. Phys.* **1996**, *105*, 8684.

(6) Zhao, Y.; Truhlar, D. G. *J. Chem. Theory Comput.* **2005**, *1*, 415.

(7) Wesolowski, T. A.; Tran, F. *J. Chem. Phys.* **2003**, *118*, 2072.

(8) Kohn, W.; Meir, Y.; Makarov, D. E. *Phys. Rev. Lett.* **1998**, *80*, 4153.

(9) Patkowski, K.; Jeziorski, B.; Szalewicz, K. *J. Chem. Phys.* **2004**, *120*, 6849.

(10) Misquitta, A.; Podeszwa, R.; Jeziorski, B.; Szalewicz, K. *J. Chem. Phys.* **2005**, *123*, 214103.

(11) Tao, J.; Perdew, J. P. *J. Chem. Phys.* **2005**, *122*, 114102.

(12) Langreth, D.; Dion, M.; Rydberg, H.; Schroder, E.; Hyldgaard, P.; Lundqvist, B. *Int. J. Quantum Chem.* **2005**, *101*, 599.

(13) Grimme, S. *J. Comput. Chem.* **2004**, *25*, 1463.

(14) Williams, R.; Malhotra, D. *Chem. Phys.* **2006**, *327*, 54.

(15) Becke, A.; Johnson, E. *J. Chem. Phys.* **2005**, *122*, 154104.

(16) Becke, A.; Johnson, E. *J. Chem. Phys.* **2005**, *123*, 154101.

(17) Johnson, E.; Becke, A. *J. Chem. Phys.* **2006**, *124*, 174104.

(18) von Lilienfeld, O. A.; Tavernelli, I.; Rothlisberger, U.; Sebastiani, D. *Phys. Rev. Lett.* **2004**, *93*, 153004.

(19) von Lilienfeld, O. A.; Tavernelli, I.; Rothlisberger, U.; Sebastiani, D. *Phys. Rev. B* **2005**, *71*, 195119.

(20) Tkatchenko, A.; von Lilienfeld, O. A. *Phys. Rev. B* **2006**, *73*, 153406.

(21) von Lilienfeld, O. A.; Andrienko, D. *J. Chem. Phys.* **2006**, *124*, 054307.

(22) Cornell, W. D.; Cieplak, P.; Bayly, C. I.; Gould, I. R.; Merz, K. M.; Ferguson, D. M.; Spellmeyer, D. C.; Fox, T.; Caldwell, J. W.; Kollman, P. A. *J. Am. Chem. Soc.* **1995**, *117*, 5179.

(23) Parameters for DCACPs were tabulated in the Supporting Information. The same procedure as in ref 29 was used to generate the DCACPs; however, the parameters for hydrogen were calibrated against the CCSD(T) reference of the H2 dimer in the parallel configuration instead of the full configuration interaction method.

(24) *CPMD;* Copyright IBM Corp 1990−2001, Copyright MPI fuer Festkoerperforschung Stuttgart 1997−2001.

(25) CPMD consortium page. http://www.cpmd.org (accessed May 5, 2007).

(26) Becke, A. D. *Phys. Rev. A* **1988**, *38*, 3098.

(27) Lee, C.; Yang, W.; Parr, R. G. *Phys. Rev. B* **1988**, *37*, 785.

(28) Goedecker, S.; Teter, M.; Hutter, J. *Phys. Rev. B* **1996**, *54*, 1703.

(29) Lin, I.-C.,; Coutinho-Neto, M. D.; Felsenheimer, C.; von Lilienfeld, O. A.; Tavernelli, I.; Rothlisberger, U. submitted to *Phys. Rev. B.* **2007**, *75*, 205131.

(30) Frisch, M. J.; Trucks, G. W.; Schlegel, H. B.; Scuseria, G. E.; Robb, M. A.; Cheeseman, J. R.; Montgomery, J. A., Jr.; Vreven, T.; Kudin, K. N.; Burant, J. C.; Millam, J. M.; Iyengar, S. S.; Tomasi, J.; Barone, V.; Mennucci, B.; Cossi, M.; Scalmani, G.; Rega, N.; Petersson, G. A.; Nakatsuji, H.; Hada, M.; Ehara, M.; Toyota, K.; Fukuda, R.; Hasegawa, J.; Ishida, M.; Nakajima, T.; Honda, Y.; Kitao, O.; Nakai, H.; Klene, M.; Li, X.; Knox, J. E.; Hratchian, H. P.; Cross, J. B.; Adamo, C.; Jaramillo, J.; Gomperst, R.; Stratmann, R. E.; Yazyev, O.; Austin, A. J.; Cammi, R.; Pomelli, C.; Ochterski, J. W.; Ayala, P. Y.; Morokuma, K.; Voth, G. A.; Salvador, P.; Dannenberg, J. J.; Zakrzewski, V. G.; Foresman, J. B.; Ortiz, J. V.; Cui, Q.; Baboul, A. G.; Clifford, S.; Cioslowski, J.; Stefanov, B. B.; Liu, G.; Liashenko, A.; Piskorz, P.; Komaromi, I.; Martin, R. L.; Fox, D. J.; Keith, T.; Al-Laham, M. A.; Peng, C. Y.; Nanayakkara, A.; Challacombe, M.; Gill, P. M. W.; Johnson, B.; Chen, W.; Wong, M. W.; Gonzalez, C.; Pople, J. A. *GAUSSIAN 03, Revision A.1*; Gaussian, Inc.: Pittsburgh, PA, 2003.

(31) Werner, H.-J.; Knowles, P. J.; Lindh, R.; Manby, F. R.; Schütz, M.; Celani, P.; Korona, T.; Rauhut, G.; Amos, R. D.; Bernhardsson, A.; Berning, A.; Cooper, D. L.; Deegan, M. J. O.; Dobbyn, A. J.; Eckert, F.; Hampel, C.; Hetzer, G.; Lloyd, A. W.; McNicholas, S. J.; Meyer, W.; Mura, M. E.; Nicklass, A.; Palmieri, P.; Pitzer, R.; Schumann, U.; Stoll, H.; Stone, A. J.; Tarroni, R.; Thorsteinsson, T. *MOLPRO, version 2006.1*; 2006.

(32) Boys, S. F.; Bernardi, F. *Mol. Phys.* **1970**, *19*, 553.

(33) Simon, S.; Duran, M.; Dannenberg, J. J. *J. Chem. Phys.* **1996**, *105*, 11024.

(34) Cox, E.; Smith, J. *Nature* **1954**, *173*, 75.

(35) Cox, E.; Cruickshank, D.; Smith, J. *Proc. R. Soc. London., Ser. A* **1958**, *247*, 1.

(36) Dacosta, P.; Nielsen, O.; Kunc, K. *J. Phys. C: Solid. State. Phys.* **1986**, *19*, 3163.

(37) Tsuzuki, S.; Luthi, H. *J. Chem. Phys.* **2001**, *114*, 3949.

(38) Johnson, E.; Becke, A. *J. Chem. Phys.* **2005**, *123*, 024101.

(39) Chickos, J.; Acree, W. *J. Phys. Chem. Ref. Data* **2002**, *31*, 537.

(40) Oliver, G. D.; Eaton, M.; Huffman, H. M. *J. Am. Chem. Soc.* **1948**, *70*, 1502.

(41) Nakamura, M.; Miyazawci, T. *J. Chem. Phys.* **1969**, *51*, 3146.

(42) Schweizer, W.; Dunitz, J. *J. Chem. Theory Comput.* **2006**, *2*, 288.

(43) Girifalco, L.; Lad, R. *J. Chem. Phys.* **1956**, *25*, 693.

(44) Benedict, L. X.; Chopra, N. G.; Cohen, M. L.; Zettl, A.; Louie, S. G.; Crespi, V. H. *Chem. Phys. Lett.* **1998**, *286*, 490.

(45) Zacharia, R.; Ulbricht, H.; Hertel, T. *Phys. Rev. B* **2004**, *69*, 155406.

(46) Sinnokrot, M. O.; Valeev, E. F.; Sherrill, C. D. *J. Am. Chem. Soc.* **2002**, *124*, 10887.

(47) The value of 38 meV/atom derived by the DCACP-MP2 approach in ref 18 refers to the interaction of two graphene sheets. For a comparison with the interlayer binding of the graphite crystal, this value has to be multiplied by a factor of 2.

(48) Baskin, Y.; Mayer, L. *Phys. Rev.* **1955**, *100*, 544.

(49) Rydberg, H.; Dion, M.; Jacobsen, N.; Schröder, E.; Hyldgaard, P.; Simak, S. I.; Langreth, D. C.; Lundqvist, B. I. *Phys. Rev. Lett.* **2003**, *91*, 126402.

CT700049S